DYNA
ISSN: 0012-7353
ISSN: 2346-2183
Universidad Nacional de Colombia

Entropy generation analysis for the design of a flat plate solar collector with fins

Muñoz, Milton; Roa, Manuel; Correa, Rodrigo
Entropy generation analysis for the design of a flat plate solar collector with fins
DYNA, vol. 87, no. 212, 2020
Universidad Nacional de Colombia
Available in: http://www.redalyc.org/articulo.oa?id=49663642024
DOI: 10.15446/dyna.v87n212.80111

Artículos

Entropy generation analysis for the design of a flat plate solar collector with fins

Análisis de la generación de entropía para el diseño de colectores solares de placa plana con aletas

Milton Muñoz [a] mmunoz@unisangil.edu.co
Fundación Universitaria de San Gil, Colombia
Manuel Roa [b] mafrara5@yahoo.es
Universidad Industrial de Santander, Colombia
Rodrigo Correa [c] crcorrea@saber.uis.edu.co
Universidad Industrial de Santander, Colombia

DYNA, vol. 87, no. 212, 2020

Universidad Nacional de Colombia

Received: 05 June 2019
Revised document received: 12 December 2019
Accepted: 12 February 2020

DOI: 10.15446/dyna.v87n212.80111

Abstract: This article describes the optimal design of a flat-plate solar collector with fins, based on the minimum entropy generation criterion. The design parameters were optimized, considering entropy generation due to heat transfer and airflow. The latter has not been considered in previous works. The flat plate in the collector is assimilated to a finned heat sink. The dimensionless entropy generation variation is analyzed to increase values of the number of fins, as well as for different plate thicknesses and heights. We also considered variations in airflow velocity. Our data shows that airflow velocity greatly influences entropy generation. Values other than the optimum found, caused a considerable growth of total entropy. For a collector area of 4 m^2, and an outlet temperature of 50°C, the optimum parameters that minimize the entropy generation rate were: 9 fins on each side of the collector plate, a height of 5 $x10^{-2}$ m, a thickness of $25x10^{-3}$m, and an air velocity variable between 0.015 and 0.046 m/s. This development is relevant to the design of flat plate solar collectors, for grain drying applications.

Keywords: entropy generation minimization, fin efficiency, flat plate solar collector, particle swarm optimization.

Resumen: Este artículo describe el diseño óptimo de un colector solar de placa plana con aletas, a partir del uso del criterio de mínima generación de entropía. Los parámetros de diseño para el colector, fueron optimizados considerando tanto la generación de entropía por transferencia de calor, como la generación de entropía debida al flujo del aire que circula por él, la cual, de manera general, no ha sido considerada en trabajos previos. La placa plana del colector fue tratada como un disipador de calor con aletas, y el valor adimensional de la variación de la entropía generada fue analizado para valores crecientes del número de aletas, de su grosor y altura, así como para diversos valores de la velocidad del flujo de aire en el colector. El estudio demuestra que esta velocidad tiene una gran influencia sobre dicho valor. Valores fuera del rango encontrado como óptimo en los diseños, ocasionan un incremento considerable de la entropía generada en el sistema. Para un área en el colector de 4 m^2, y una temperatura de salida de 50°C, los parámetros óptimos que minimizan la entropía generada, fueron 9 aletas por cada cara de la placa del colector, con una altura de 5 $x10^{-2}$ m, un grosor de $25x10^{-3}$m, y una velocidad del aire variable entre 0.015 y 0.046 m/s. El estudio desarrollad es de gran relevancia para el diseño de colectores solares de placa plana, en aplicaciones destinadas al secado de granos.

Palabras clave: colector solar de placa plana, eficiencia de aleta, minimización de entropía generada, optimización por enjambre de partículas.

1. Introduction

Entropy generation minimization in a system (EGM), has been used as an optimization strategy, and has been endorsed and implemented in various fields of engineering over the last decades. Adrian Bejan, precursor and diffuser of the method, affirms the foundation for EGM is the theorem of Gouy-Stodola [1]. According to this theorem, the work lost or not available in a system is defined by eq. (1), in which T_o is the reference temperature of the system, and $\#_{gen}$ the variation of its entropy generated with time.

$$W_{lost} = T_o \dot{S}_{gen} \tag{1}$$

In this way, minimizing $\#_{gen}$ involves minimizing lost or unavailable work. In other words, minimizing $\#_{gen}$ makes the system less irreversible, and therefore, thermodynamically optimal. A detailed description of what entropy is and what entropy is not and the generation of entropy, can be read in [2]. On the other hand, EGM as a design method is clearly detailed in [3], and in [4]. An application of EGM to systems that simultaneously combine mass and heat transfer is exemplified in [5].

The need to take full advantage of renewable solar energy has made the use of EGM in the design of solar collectors recurrent (see Fig. 1). From the application of the second law of thermodynamics, [6] estimated as promising areas for fossil fuels to be displaced by solar energy, those whose entropy was comparable with the entropy of the systems that convert solar energy into hot. Kreider notes that, in effect, fossil fuels are sources of low entropy, generally employed in high entropy applications. Subsequently, Bejan performs a detailed analysis of the EGM in isothermal and non-isothermal solar collectors [7], in which a dimensionless expression is defined for the variation of the entropy generated, based on entry and exit temperatures, and the maximum temperature of the collector. This showed that minimizing the entropy generated in a solar collector is equivalent to maximizing its exergy flow. Therefore, [8], considering this fact, optimized the model of different types of solar heaters, by maximizing their exergy balance [9].

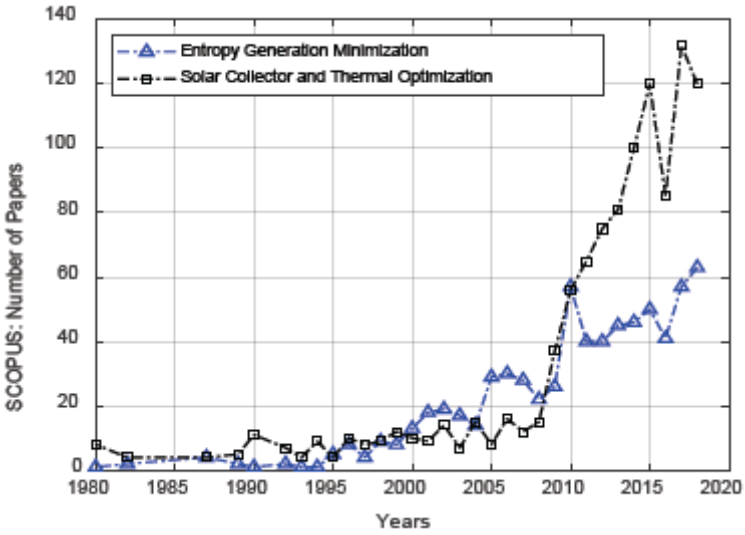

Figure 1
SCOPUS publications referents to EGM and to Solar Collector and Thermal Optimization.
Source: The Authors.

Otherwise, [10], apply the EGM to optimize the design of a grain solar dryer, with natural air circulation. An analysis similar to that developed by Bejan is also presented in [11] by Saha, and in [12] by Torres. In other works of Torres, there are two additional developments: one explores the application of the EMG in solar collectors for drying processes [13], and another explores the application of the EMG to determine the temperature and length of the optimal fluid conduit channel, in solar collectors of different configurations [14]. More recently, several works have studied the efficiency and optimization of flat-plate solar collectors, too. Some examples include [15] and [16]. Others include [17] and [18], where the authors focused on analyzing the effect of airflow orientation. They also studied how the geometry of plate fins influences the process. They found that using a counter flow and a corrugated absorber makes the process more efficient. Other works have also shown that it is better to use a flat plate with fins rather than a smooth one, and that the number of fins strongly influences exergy maximization [19,20,21].

This work explores the influence of plate geometry in thermal optimization, considering two variation sources for the entropy generation rate: heat transfer and airflow velocity. Considering that despite the number of published works, the effect of airflow velocity is yet to be addressed, including the latter is paramount, as this variable directly influences air temperature regulation at the output of the collector, depending on different values of solar irradiance. This is the main research objective and the principal contribution of this paper.

We treated the flat plate in the collector as a finned heat sink. We varied airflow velocity, and also, we analyzed dimensionless entropy variation for an increasing number of fins, as well as for different fin thicknesses and heights. This work synthesizes the design method for a solar collector that minimizes entropy generation rate. Such results are important for future applications, e.g. related to solar grain drying. In this article the

entropy generation model is presented along with the equations that define the design of a fin with a constant cross section. Then, in the results section, the optimization problem is developed by means of PSO (Particle Swarm Optimization). Finally, some of the most relevant conclusions are presented.

2. Methods and modeling

The logical sequence followed in the present work, entailed:

- Calculation of the variation of the entropy generated in a flat plate solar collector.
- Determination of the drag force of the airflow in the collector, from the calculation of the Reynolds number.
- Determination of the heat transfer coefficient for the airflow in the collector, from the calculation of the Nusselt number.
- Metaheuristic optimization of the variation of the entropy generated, and determination of the values corresponding to the quantity, thickness and height of the fins in the collector, as well as the velocity of the surrounding flow, which minimize the variation of the entropy generated.
- Simulation of the variation of the entropy and the efficiency in the collector, with respect to the variation of the number, thickness and height of the fins, and the velocity of the flow.

The mathematical expression for the dimensionless variation of the entropy generated in the collector is broken down below.

2.1. Entropy models generated in a non-isothermal flat plate solar collector

The entropy balance in a system is defined in [22] as,

$$S_{heat} + S_{mass} + S_{gen} = \Delta S_{system} \tag{2}$$

From the above equation, we can express the velocity of the variation of the entropy generated in the collector as,

$$\dot{S}_{gen} = \frac{dS_{system}}{dt} - \dot{S}_{heat} - \dot{S}_{mass} \tag{3}$$

This entropy generated velocity of variation is therefore composed of three parts: the variation of entropy in the system, the variation of entropy by heat transfer, and the variation of entropy by mass flow (which, for the case of the collector, is air). Each component is described below.

2.1.1. Variation of entropy in the system

The variation of entropy in the system is caused by the non-isothermal condition of the metal plate in the collector. According to the first law of thermodynamics, the internal energy of a system in which heat generates work is defined by,

$$dU=\delta Q-\delta W \tag{4}$$

The variation of entropy in the system is given by,

$$dS=\frac{dQ}{T} \tag{5}$$

Therefore, from the two previous equations, and keeping in mind that the work generated is equal to the product pressure by volume (PdV), we have to,

$$dS=\frac{dU}{T}+\frac{PdV}{T} \tag{6}$$

In the collector, the variation of the internal energy dU, is proportional to the variation of the temperature in its plate, according to the following equation:

$$dU=mc_v dT \tag{7}$$

with m equal to the mass of air that circulates through the collector, and c_v to its specific heat. On the collector, there is no variation in volume, so that dS can be defined as,

$$dS=mc_v\frac{dT}{T} \tag{8}$$

When integrating, you get that,

$$\Delta S=mc_v \ln\left(\frac{T_{out}}{T_{in}}\right) \tag{9}$$

Therefore, the velocity of variation of the entropy in the system is,

$$\frac{dS}{dt}=\dot{m}c_v \ln\left(\frac{T_{out}}{T_{in}}\right) \tag{10}$$

2.1.2. Variation of entropy by heat transfer

The variation of the entropy by heat transfer is given by the solar radiation, and by the heating of the air that enters the collector from the outside (caused precisely by said radiation). This can be expressed as,

$$S_{heat} = \frac{Q_{sun}}{T_{sun}} - \iint \frac{q_0}{T_0} dA = \frac{Q_{sun}}{T_{sun}} - \frac{Q_0}{T_0} \tag{11}$$

being, Q_{sun} and Q_0, the heat of the sun and of the air, respectively. From the above equation, we get that,

$$\dot{S}_{heat} = \frac{\dot{Q}_{sun}}{T_{sun}} - \frac{\dot{Q}_0}{T_0} \tag{12}$$

with T_0 equal to the ambient temperature. Q_{sun} is proportional to the product of the average solar radiation (G, Wm^{-2}), by the area of the collector,

$$\dot{Q}_{sun} = GA_c(\tau\sigma) \tag{13}$$

with, $\tau\sigma$ equal to the absorbance product of the transmittance in the collector.

2.1.3. Variation of entropy by mass flow

The variation of entropy by mass flow is due to the flow of air that circulates through the collector. This variation is defined as,

$$S_{mass} = m(s_{in} - s_{out}) \tag{14}$$

The variation of the enthalpy in this airflow is given by,

$$dh = du + dw = Tds + \frac{1}{\rho}dP \tag{15}$$

Therefore,

$$h_{out} - h_{in} = T(s_{out} - s_{in}) + \frac{1}{\rho}(P_{out} - P_{in}) \tag{16}$$

and considering the enthalpy variation close to zero, it is determined that,

$$(s_{out} - s_{in}) = -\frac{1}{\rho T}(P_{out} - P_{in}) \tag{17}$$

Consecuently,

$$\dot{S}_{mass} = -\frac{\dot{m}}{\rho T}(P_{out} - P_{in}) = -\frac{F_d V_f}{T} \tag{18}$$

where, T, F_d and V_f are the temperature, force and the average velocity of the air, respectively.

2.1.4. Entropy generation

Based on the above definitions, the rate of entropy variation in the isothermal collector is defined by,

$$\dot{S}_{gen} = \dot{m}c_v \ln\left(\frac{T_{out}}{T_{in}}\right) + \frac{\dot{Q}_0}{T_0} - \frac{\dot{Q}_{sun}}{T_{sun}} + \frac{F_d V_f}{T} \tag{19}$$

From a general energy balance, $\dot{Q}_0$ is

$$\dot{Q}_0 = \dot{Q}_{sun} - \dot{Q}_c \tag{20}$$

$\dot{Q}_c$ can be expressed as a function of the temperature delta in the plate, starting from the differential equation that defines the energy balance in the collector,

$$q_{sun} = q_{air} + \dot{m}c_v \frac{dT_c}{dA} \tag{21}$$

hence it will have that,

$$\dot{Q}_c = \dot{m}c_v(T_{out} - T_{in}) \tag{22}$$

$\#_{gen}$ can then be written as,

$$\dot{S}_{gen} = \dot{m}c_p \ln\left(\frac{T_{out}}{T_{in}}\right) + \frac{\dot{Q}_{sun} - \dot{m}c_v(T_{out} - T_{in})}{T_0} - \frac{\dot{Q}_{sun}}{T_{sun}} + \frac{F_d V_f}{T} \tag{23}$$

$$\dot{S}_{gen} = \frac{\dot{Q}_{sun}(T_{sun} - T_0)}{T_o T_{sun}} + \frac{F_d V_f}{T} - \frac{\dot{m}c_v(T_{out} - T_{in})}{T_0} + \dot{m}c_v \ln\left(\frac{T_{out}}{T_{in}}\right) \tag{24}$$

If the definition proposed by Bejan is used for dimensionless entropy variation, Ns,

$$N_s = \frac{\dot{S}_{gen} T_0}{\dot{Q}_{sun}} \tag{25}$$

and if it is used,

$$M = \frac{\dot{m}c_v T_0}{\dot{Q}_{sun}} = \frac{\dot{m}c_v T_0}{GA_c(\tau\sigma)} \tag{26}$$

$$\theta_{in} = \frac{T_{in}}{T_0}, \quad \theta_{out} = \frac{T_{out}}{T_0}, \; \theta_{sun} = \frac{T_{sun}}{T_0} \tag{27}$$

$$B = \frac{1}{GA_c(\tau\sigma)} \tag{28}$$

results that,

$$N_s = 1 - \frac{1}{\theta_{sun}} + BF_d V_f + M\left(\ln\left(\frac{\theta_{out}}{\theta_{in}}\right) - \theta_{out} + \theta_{in}\right) \tag{29}$$

M is found from the differential equation of the energy balance in the collector. Solving this differential equation, we obtain that,

$$M = \left[(\theta_{max} - 1)\ln\left(\frac{\theta_{max} - \theta_{in}}{\theta_{max} - \theta_{out}}\right)\right]^{-1} \tag{30}$$

where θ_{max} is the maximum temperature that the collector can reach, which is determined by solving the energy balance in the collector, too. This is defined in a dimensionless way, like,

$$\theta_{max} = 1 + \frac{GA_c(\tau\sigma)}{hA_p T_0} = 1 + \frac{\dot{Q}_{sun}}{hA_p T_0} \tag{31}$$

In the definition of θ_{max}, h is equal to the heat transfer coefficient of the air in the collector, and A_p equal to the heat transfer area in the collector (area of the metal plate), which is at least twice the area of the collector, if a plate without fins is considered. In effect, A_p will increase with the number of fins on the plate.

2.2. Geometry of the Plate of the Collector

The geometry of the collector plate is associated with the expression to find Ns, in the calculation of the drag force (which depends on the Reynolds number), of the air velocity, and in the calculation of h (which depends on the number of Nusselt). The procedure is similar to the developments made for finned heat sinks, such as those presented by [23]-[27].

On a plate in the collector, with rectangular fins on both sides of the plate, with dimensions of the plate as shown in the above figure, (See Fig. 2). Here, the area of the collector A_{cl}, the area of the plate without fins, A_{unfin} , the perimeter of the base of the fin, p, the area of the base of the fin,

A_{bI}, the space between fins, s, and the number of fins, N, are determined by the following expressions,

$$A_c = WL \tag{32}$$

$$p = 2t_{fin} + 2L \tag{33}$$

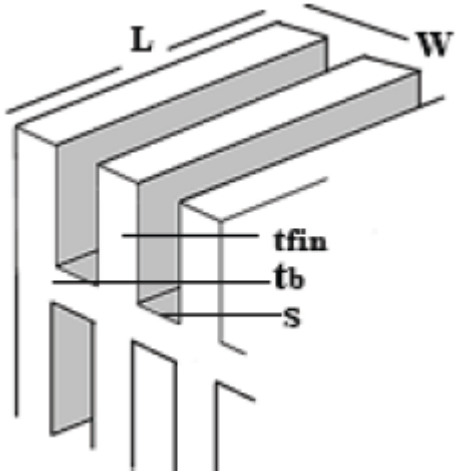

Figure 2
Fin geometry in the collector plate
Source: The Authors.

$$A_b = t_{fin}L \tag{34}$$

$$A_{unfin} = 2WL - 2Nt_{fin}L \tag{35}$$

$$s = \left(\frac{W - t_{fin}}{N - 1}\right) - t_{fin} \tag{36}$$

$$4 \leq N \leq 2\text{int}\left[1 + \left(\frac{N - t_{fin}}{t_{fin}}\right)\right] \tag{37}$$

The drag force is defined as,

$$F_d = \rho V_{ch}{}^2\left(f_{app}N(2HL + sL) + K_cHW + K_eHW\right) \tag{38}$$

where, V_{ch}, is the velocity of the channel, f_{app} the apparent friction factor (for laminar flow, which depends on the value of the Reynolds number, Re_{Dh}), K_c the apparent contraction factor, and K_e the expansion factor apparent, which are defined as follows:

$$V_{ch} = V_f\left(1 + \frac{t_{fin}}{s}\right) \tag{39}$$

$$f_{app} = \left[\left(\frac{3.44}{Re_{Dh}\sqrt{L^*}}\right)^2 + (f)^2\right]^{1/2} \tag{40}$$

$$Re_{Dh} = \frac{D_h V_{ch}}{\nu} \tag{41}$$

$$D_h = \frac{4sH}{2s + sH} = \frac{A_t}{p_t} \tag{42}$$

$$L^* = \frac{L}{D_h Re_{Dh}} \tag{43}$$

$$f = \frac{1}{Re_{Dh}}\left(24 - 32.527\left(\frac{s}{H}\right) + 46.721\left(\frac{s}{H}\right)^2 - 40.829\left(\frac{s}{H}\right)^3 + 22.954\left(\frac{s}{H}\right)^4 - 6.089\left(\frac{s}{H}\right)^5\right) \tag{44}$$

$$K_c = 0.42(1 - \sigma^2) \tag{45}$$

$$K_e = (1 - \sigma^2)^2 \tag{46}$$

$$\sigma = 1 - \frac{Nt_{fin}}{W}$$

(47)

Re $_{Dh}$ is the Reynolds number for the hydraulic diameter of the channels that form the fins (D_h), and ν the viscosity of the fluid that circulates through the collector (air). The value of the heat transfer coefficient, h, is cleared from the Nusselt number, using the following equations,

$$N_{ub} = \frac{h * s}{k_f} \tag{48}$$

$$N_{ub} = \left[\left(\frac{P_r Re_s^*}{2} \right)^{-3} + \left(0.664 P_r^{1/3} \sqrt{Re_s^*} \sqrt{1 + \frac{3.65}{\sqrt{Re_s^*}}} \right)^{-3} \right]^{1/3} \tag{49}$$

$$Re_s^* = Re_s \frac{s}{L} = \frac{s * V_{ch}}{\nu} \left(\frac{s}{L} \right) \tag{50}$$

being, Pr the number of Prandtl, which for the air is approximately 0.7. The parameter k_f is the thermal conductivity of the air, and Re_s the Reynolds number for the spacing s, between the fins of the plate. On the other hand, θ_{max} depends on h and Ap, the heat transfer area, which is equal to:

$$Ap = A_{unfin} + A_{fin} + A_{bp} \tag{51}$$

being A_{unfin}, A_{fin}, A_{bp}, the area of the plate without fins (eq. (35)), the area of the fins (eq. (52)), and the area of the base of the plate on which the fins are mounted (eq. (53)), respectively.

$$A_{fin} = 2N(2LH + t_{fin}L + 2t_{fin}H) \tag{52}$$

$$A_{bp} = (2t_b W + 2t_b L) \tag{53}$$

Now, using the global optimization method PSO (Particle Swarm Optimization), we will find the values of V_f, N, t_{fin}, and H, which

minimize Ns, for a desired output temperature value (θ_{out}), taking as fixed values B, θ_{in}, and k_f. It should be noted that θ_{max} can also be expressed as,

$$\theta_{max} = 1 + \frac{GA_c(\tau\sigma)}{RT_0} \tag{54}$$

where R is the thermal resistance of the collector plate, understood as a heat sink. The product hA_p, in fact, must be equal to said resistance, which can be determined from the thermal dynamics of the dissipator. In a flat plate solar collector with fins, at the base of each fin (with base area equal to A_b) it is satisfied that,

$$\dot{Q}_c = \left(-kA_b \frac{dT}{dx}\middle| x = 0\right) \tag{55}$$

In other respect, the differential equation that governs the heat transfer in each fin is, in turn,

$$\frac{d}{dx}\left(kA_b \frac{dT}{dx}\right) - hp(T - T_0) = 0 \tag{56}$$

h being equal to the heat transfer coefficient of the air by convection (W/m^2 K), and k the coefficient of heat transfer by conduction of the material from which the collector plate is made (W/m K). In a solar collector with flat plate and rectangular fins, whose length is equal to the length of the base of the plate, starting from the two previous equations, for a flat collector with N fins of constant transversal area, it can be demonstrated that, for the collector, the energy balance establishes that,

$$\dot{Q}_c = \left[\frac{1}{hA_{unfin} + 2N\sqrt{hpkA_b}\tanh(aH)} + \frac{b}{kA_c}\right]^{-1} (T_{out} - T_{in}) \tag{57}$$

where b is the thickness of the plate, and a is defined by the following equation,

$$a = \sqrt{\frac{hp}{kA_b}} \tag{58}$$

R therefore, is equal to,

$$R = \frac{1}{hA_{unfin} + 2N\sqrt{hpkA_b}\tanh(aH)} + \frac{b}{kA_c} \quad (59)$$

3. Analysis of results

The parameters shown in Table 1 were considered for a collector with an aluminum plate, and a desired outlet temperature of 50°C. This temperature was selected, because it is required for grain drying applications, such as coffee or cocoa.

Table 1
Parameters of flat plate solar collector with fins.

Parameters	Symbol	Value
Collector length	L	2 m
Collector width	W	2 m
Metallic base thickness	t_b	2/1000 m
Thermal conductivity (Al)	k	230 W/m K
Solar radiation	G	300 W/m^2
Sun's apparent temperature	T_{sun}	4500 K
Ambient Temperature	T_0	296 K
Thermal conductivity (air)	k_f	0.0267 W/m K
Density (air)	P	1.177 kg/m^3
Kinematic viscosity coefficient (air)	ν	1.6 x10^{-5} m^2/s
Prandtl number (air)	P_r	0.7

Source: The Authors.

Starting from these parameters, and by means of a particle swarm optimization algorithm, PSO, we found the values for N, V_f, t_{fin} and H, which minimize the entropy generation number, Ns (eq. (29)). The results of the minimization appear in Table 2. N represents the number of fins by one side of the plate in the collector. The total fins in the collector are 2N.

Table 2
PSO parameters and optimization results

PSO Parameters		
Maximum number of function evaluations		500.000
Function evaluation		7300
Number of particles		100
Tolerance		1e-20
Searching Interval	N	[2 - 33]
	V_f	[0.00008 - 1] m/s
	t_{fin}	[1 - 25] m x 10^{-3}
	H	[1 - 5] m x 10^{-2}
Computation time		0.8107 s
Optimization Results		
	N	6
	V_f	0.015 m/s
	t_{fin}	25 m x 10^{-3}
	H	5 m x 10^{-2}

Source: The Authors.

These results were obtained assuming an irradiance of 300 W/m^2, with an input temperature of 23°C. With this, and the values of N, V_f, t_{fin}, and H, the collector can reach an outlet temperature of 50°C. Nevertheless, this must be confirmed. From the energy balance in the collector (eq. (21)), it was possible to establish that, indeed, for parameters found, outlet temperature reaches 50°C (see Fig. 3). But irradiance varies during the day. For this reason, the optimization method must carry out tests with different values of irradiance and input temperature in the collector. Also, from eq. (21), the minimum air velocity required to reach 50°C at the output of the collector was fixed. We ran the optimization algorithm again. The new results are summarized in Table 3.

Table 3
Optimization results for different values of g and tin

G [W/m_2]	T_{in} [°C]	N	H [m x10^{-2}]	t_{fin} [m]	V_f [m/s]
382.81	24.31	7	5	0.025	0.019
580.13	27.17	8	5	0.025	0.032
653.68	29.30	8	5	0.025	0.040
728.63	29.86	9	5	0.025	0.046
709.57	30.30	9	5	0.025	0.046
625.16	30.09	8	5	0.025	0.040
496.77	29.26	8	5	0.025	0.030
341.95	28.18	7	5	0.025	0.020

Source: The Authors.

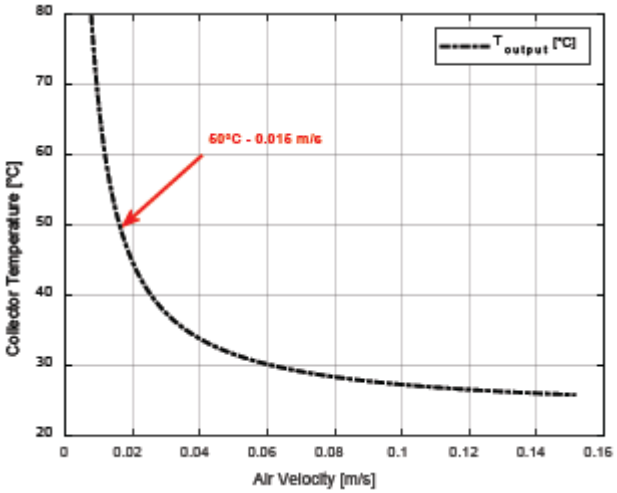

Figure 3
Outlet Temperature variation with air velocity (T_{in}, 23°C; G, 300 W/m^2, N=12, H=5mx10^{-2}, t_{fin}=25x10^{-3})
Source: The Authors.

The variation of irradiance implies variations in the number of fins, N, and the velocity of the air, V_f, while H and t_{fin} remain constant. With the objective of examining the variation of entropy generation with variable numbers of N, V_f, t_{fin}, and H, and for complementing the information of Table 3, Figs. 5-8 shows the variation of the dimensionless value of the entropy generated (eq. (29)), for variant values of these parameters, respectively.

The analyses performed allowed us to appreciate how the variation of the entropy generated in the collector, is minimized for a specific number of values of N, V_f, t_{fin} and H. For N, V_f, and t_{fin}, there is a value for which before and after the same, the entropy generated is increasing. Note that, for each parameter, Ns have a delimited range where its value is minimum, except for H. The entropy generated is stable for values of H greater than 2.5x10^{-2} m. Variation of fin thickness shows the minimum contribution to Ns respect to the contribution of N, H, and V_f, although they have an absolute minimum near to 25mm.

A typical curve of mean irradiance is shown in Fig. 4. The outlet temperature was determined from eq. (21).

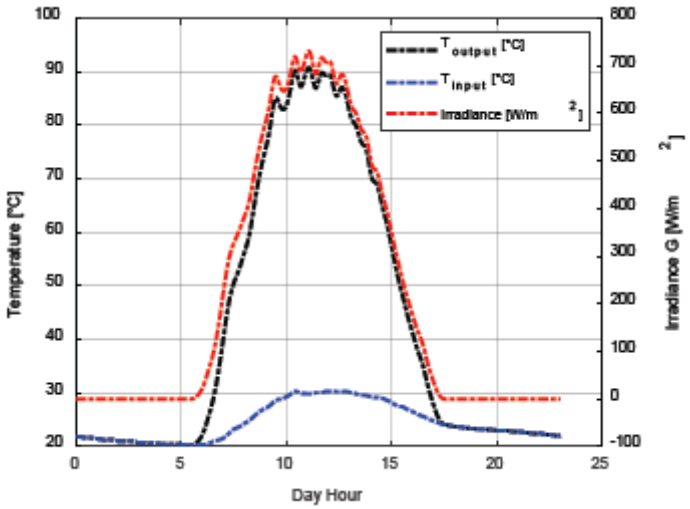

Figure 4
Irradiance and environment temperature (T_{in}), for the month of March in Bucaramanga, Colombia. (T_{output} was calculated from eq. (21), with N=6, N=12, H=5mx10^{-2}, t_{fin}=25x10^{-3})
Source: The Authors.

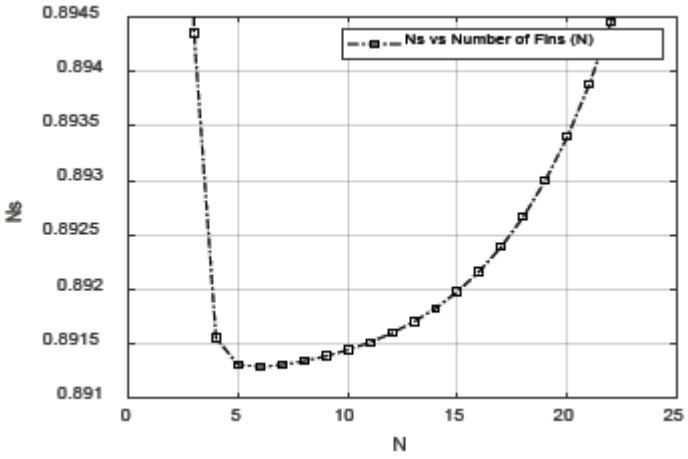

Figure 5
Variation of entropy generation number, Ns, respect to the number of fins, N, in the collector plate.
Source: The Authors.

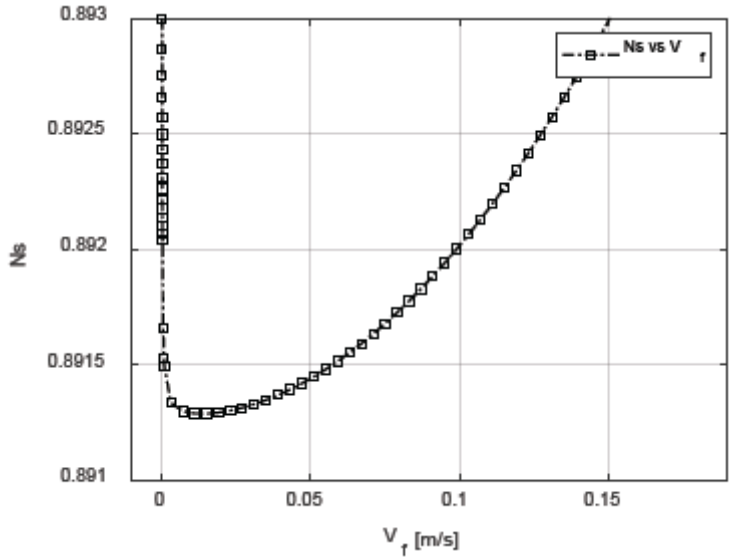

Figure 6
Variation of entropy generation number, Ns, respect to the air velocity V_f.
Source: The Authors.

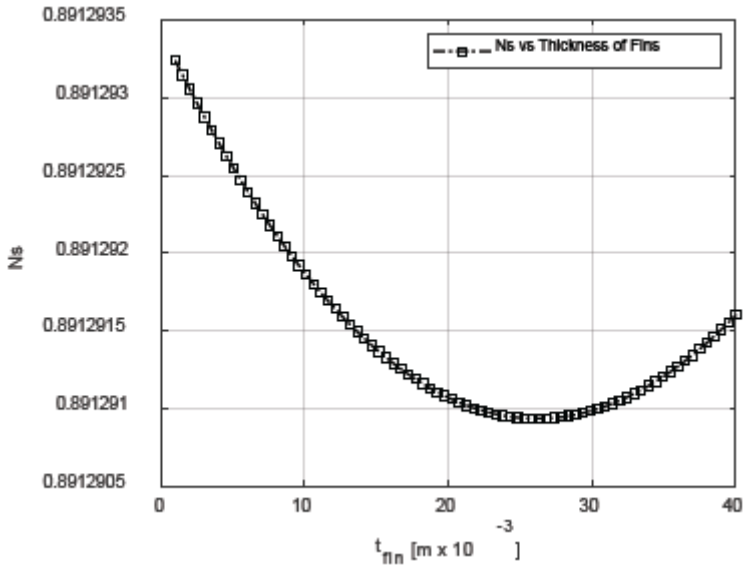

Figure 7
Variation of entropy generation number, Ns, respect to the thickness of the fins, t_{fin}
Source: The Authors.

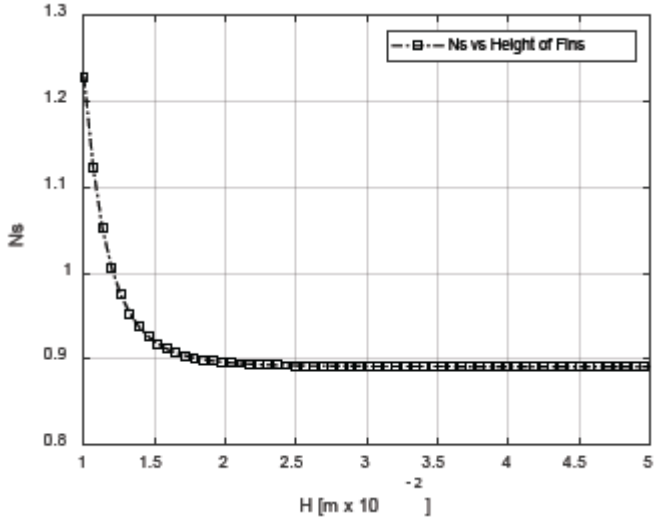

Figure 8
Variation of entropy generation number, Ns, respect to the height of the fins, H.
Source: The Authors

Figs. 9-14 show the variation of the entropy generation number (Ns), for the combinations of two geometric parameters of the plate in the collector: N and V_f, N and t_{fin}, N and H, V_f and t_{fin}, V_f and H, t_{fin} and H. These figures reveal that the most influential parameters are the number of fins (N), and the air velocity (V_f). In each pair of combinations, these parameters are dominant. When N and V_f and N and t_{fin} vary, the dominant parameter on the variation of entropy generated is N, in so much that when N and H vary. By varying V_f and t_{fin} and V_f and H, the dominant parameter is V_f. When t_{fin} and H vary, the dominant parameter is H. An optimum value for air velocity must be small (minor than 0.05 m/s), but not near zero.

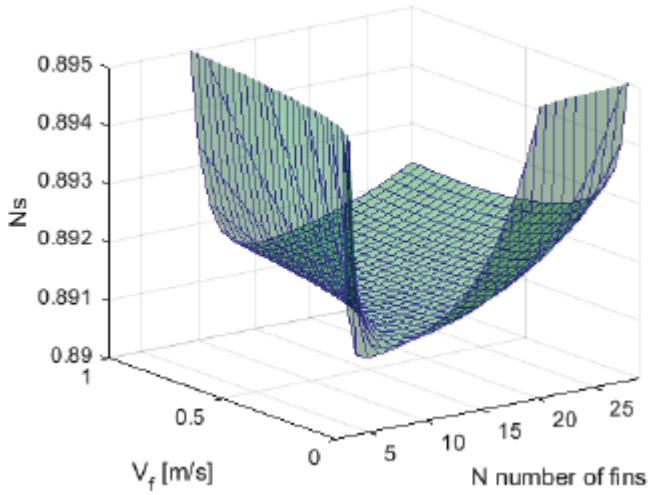

Figure 9
Variation of entropy generation number, Ns, respect to N y V_f
Source: The Authors.

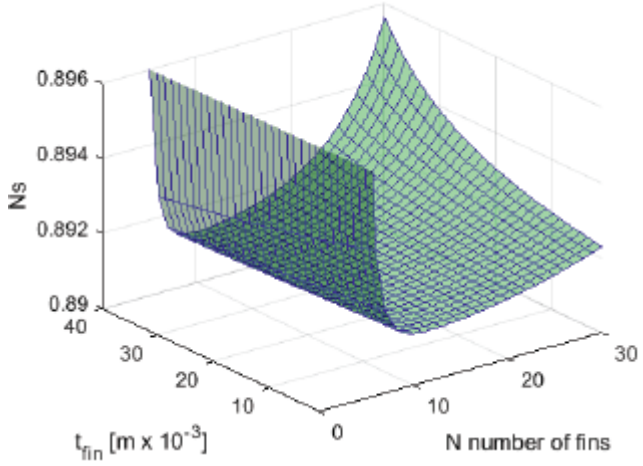

Figure 10
Variation of entropy generation number, Ns, respect to N and t_{fin}
Source: The Authors.

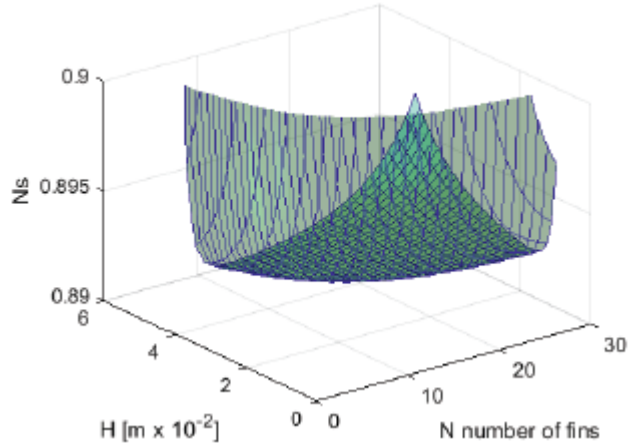

Figure 11
Variation of entropy generation number, Ns, respect to N and H
Source: The Authors.

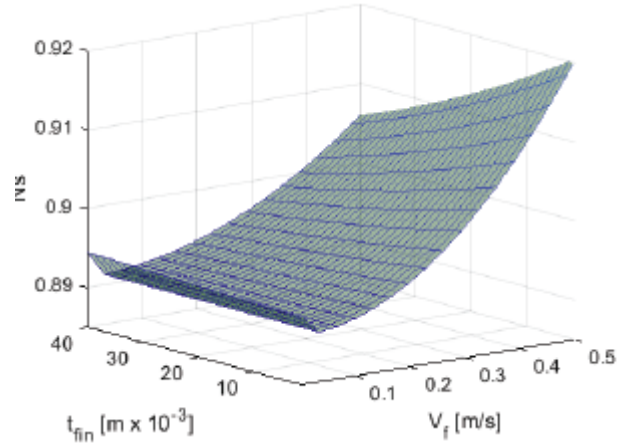

Figure 12
Variation of entropy generation number, Ns, respect to V_f and t_{fin}
Source: The Authors.

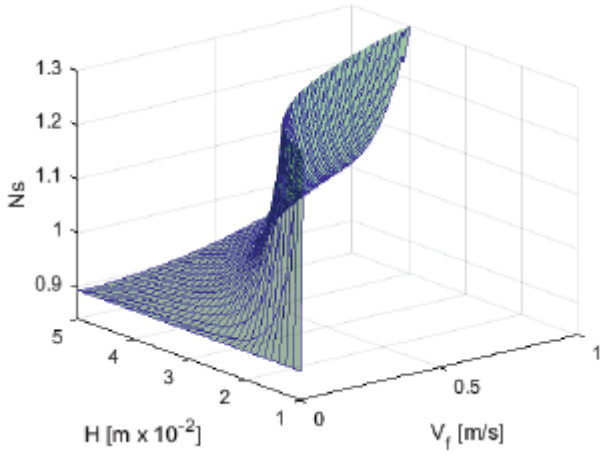

Figure 13
Variation of entropy generation number, Ns, respect to V_f and H
Source: The Authors.

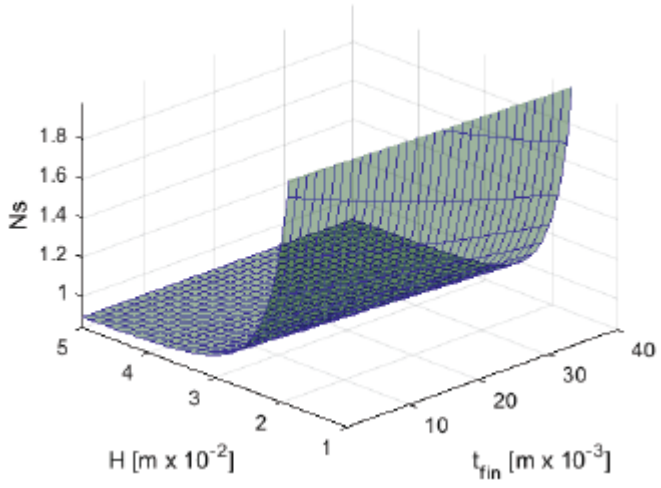

Figure 14
Variation of entropy generation number, Ns, respect to t_{fin} and H.
Source: The Authors.

The same consideration applies to the number of fins. A small number of fins (between six and nine) produces small Ns. A collector without fins is less thermally efficient evidently than a one with fins.

The efficiency of the collector plate was calculated using the ratio of the plate heat transfer with fins to plate the heat transfer without fins. We analyzed the effects of N, V_f, $t_{fin,}$ and H. The following equation was used being $\mathbf{A}_{\text{no fin}}$ equal to the area of the collector plate (without fins), [28]

$$\varepsilon_{\text{fin overall}} = \frac{\dot{Q}_{\text{total fin}}}{\dot{Q}_{\text{total no fin}}} = \frac{2N\dot{Q}_c + h(A_{\text{unfin}} + A_{\text{bp}})(T_{\text{out}} - T_{\text{in}})}{hA_{\text{no fin}}(T_{\text{out}} - T_{\text{in}})} \quad (60)$$

For variations of V_f and $t_{fin,}$ the global efficiency of the fin was found to be constant (about 1.3). This indicates that amplifying V_f or t_{fin} does not improve the collector heat transfer performance. For variations of N between 2 and 30, the global efficiency changed between 1 and 2. For N equal to 7, the global efficiency was equal to 1.3. A similar situation occurs with the variation of H between $1x10^{-2}$ m and $5x10^{-2}$ m. For these values, the global efficiency changed between 1 and 1.23. On average, this collector efficiency was 1.3, which means that the performance of the collector heat transfers with added fins, is about 30% better than that of a collector without them. This effectiveness could be increased by increasing N, but this directly affects the energy quality, because increasing N implies rising the entropy generation rate.

From simulations, the definition of R, the thermal resistance of the collector plate, with rectangular fins (eq. (59)), and the inverse of the product between the heat transfer coefficient, h, and the effective area of heat transfer, A_p, $(hA_p)^{-1}$, where compared. While increasing values of N, t_{fin}, and H, reduces the value of R, increasing values of V_f increases R. Since Reynolds's number gets larger with V_f, the rise of R with V_f is associated with the turbulence of the airflow. The values of the thermal resistance of the plate in the solar collector are comparable with the product $(hA_p)^{-1}$, for different values of N and V_f. For variations of H, R and the product $(hA_p)^{-1}$ maintains a constant difference of 0.5 [K/W]. For increasing variations of the thickness, both, the product $(hA_p)^{-1}$ and R-value decrease, but their slopes are different. Therefore, taking into account the detailed differences, these values (R and $(hA_p)^{-1}$) could be interchangeable in the equations that model the system. Figs. 15-16 show the variations of R and $(hA_p)^{-1}$ with N and Vf. The design method for a solar collector that minimizes entropy generation rate is synthesized in Table 3.

Table 3
Synthesis of the design methodology for a solar collector that minimizes entropy generation rate

Function Solar Collector Design by EGM Returns Optimum parameters that minimize Ns
Inputs: Collector area (L, W), metallic base parameters (B, K), environmental variables (G, Tsun, To), air parameters (kf, P, Pf, v)
Do: 1. **Entropy balance**. Find an expression for the variation of the generated entropy. Normalize (Ns) 2. **Establish a relationship of Ns with the geometry of the system**. Relationship of air drag force as a function of Reynolds number, and of air transfer coefficient (h) as a function of Nusselt number. 3. **Define** geometric parameters and variables that must be calculated to minimize Ns: N, tfin, H, Vf ... 4. **Apply** an optimization method: $(N, tfin, H\ y\ Vf.) \leftarrow OPTIMIZE\ (minimize\ Ns)$ 5. **Verify** results with the system power model. $T\_c \leftarrow System\ Model\ (N, t\_fin, H, V\_f)$ **If** Tc is not equal to the desired value adjust optimization ranges and **go to** 4. 6. **Repeat 4. and 5.** for different radiation values and inlet temperatures

Source: The Authors.

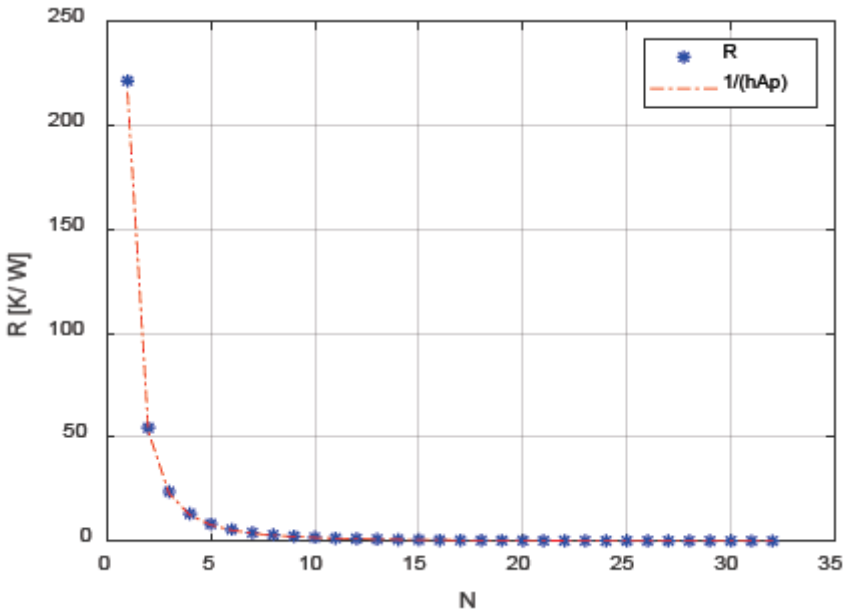

Figure 15
R and product $(hA_p)^{-1}$ for variations of N
Source: The Authors.

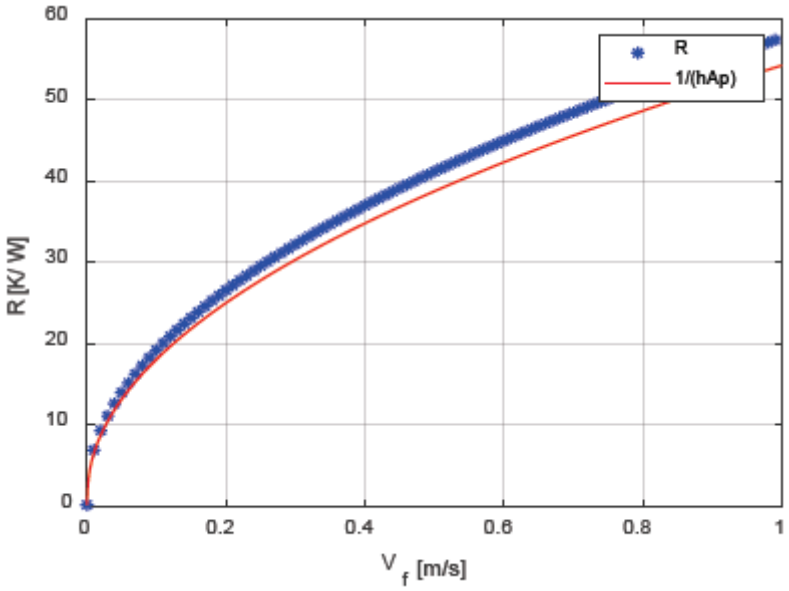

Figure 16
R and product $(hA_p)^{-1}$ for variations of V_f
Source: The Authors.

4. Conclusions

Our data demonstrated that airflow velocity within the collector greatly influences entropy generation. Nonetheless, and to the best of our knowledge, this is the first work that considers such a variable. We found that non-optimum values considerably increase entropy generation at the collector.

Moreover, our simulation of the solar collector showed that plate effectiveness increases with the number of fins and their height, but this entails a considerable growth of entropy generation. Similarly, increasing flow velocity also raises entropy generation. However, it does not increase effectiveness.

As a test case of our methodology, we determined the optimal parameters for a flat-plate solar collector. We assumed a collector with an area of 4 m^2 which receives a variable 200 and 700 W/m^2 irradiance. Our workflow revealed that the collector must contain 18 fins with a thickness of $25x10^{-3}$ m and a height of $5x10^{-2}$ m. These fins should be evenly split on each face of the collector. Our results are relevant for future developments of solar collectors. For example, the design shown can be used for grain drying processes.

References

[1] Bejan, A., The method of entropy generation minimization, Energy and the Environment, 15, in: Bejan.A., K.D.G. and Vadász, P., Ed., Environmental Science and Technology Library. Springer, Dordrecht, 1999, pp. 11-22. DOI: 10.1016/S0035-3159(96)80059-6

[2] Martyushev, L., Entropy and entropy production: old misconceptions and new breakthroughs, Entropy, 15(4), pp. 1152-1170, 2013. DOI: 10.3390/e15041152

[3] Sciacovelli, A., Verda, V. and Sciubba, E., Entropy generation analysis as a design tool - A review, Renew. Sustain. Energy Rev., 43(December), pp. 1167-1181, 2015. DOI: 10.1016/j.rser.2014.11.104

[4] Bejan, A., Advanced Engineering Thermodynamics, 4th ed., John Wiley & Sons, Inc., Hoboken, NJ, USA, 2016.

[5] Prakash, G., Lienhard, J. and Zubair, S., Entropy generation minimization of combined heat and mass transfer devices, Int. J. Therm. Sci., 49(10), pp. 2057-2066, 2010. DOI: 10.1016/j.ijthermalsci.2010.04.024

[6] Kreider, J.A.N.F., Second-Law analysis of solar-thermal processes, Energy Res., 3(February), pp. 325-331, 1979. DOI: 10.1002/er.4440030403

[7] Bejan, A., Kearney, D.W. and Kreith, F., Second Law analysis and synthesis of solar collector systems, J. Sol. Energy Eng., 103(1), pp. 23-28, 1981. DOI: 10.1115/1.3266200

[8] Altfeld, K., Leiner, W. and Fiebig, M., Second law optimization of flat-plate solar air heaters. Part I: the concept of net exergy flow and the modeling of solar air heaters, Sol. Energy, 41(2), pp. 127-132, 1988. DOI: 10.1016/0038-092X(88)90128-4

[9] Altfeld, K., Leiner, W. and Fiebig, M., Second law optimization of flat-plate solar air heaters. Part 2: results of optimization and analysis of sensibility to variations of operating conditions, Sol. Energy, 41(4), pp. 309-317, 1988. DOI: 10.1016/0038-092X(88)90026-6

[10] Onyegegbu, S.O., Morhenne, J. and Norton, B., Second Law optimization of integral type natural circulation solar energy crop dryers, Energy Convers. Manag., 35(11), pp. 973-983, 1994. DOI: 10.1016/0196-8904(94)90028-0

[11] Saha S.K. and Mahanta, D.K., Thermodynamic optimization of solar flat-plate collector, Renew. Energy, 23, pp. 181-193, 2001. DOI: 10.1016/S0960-1481(00)00171-3

[12] Torres, E., Cervantes-de Gortari, J.C., Ibarra, B.A. and Picon, M., A design method of flat-plate solar collectors based on entropy generation minimization, Exergy, 1(1), pp. 46-52, 2001. DOI: 10.1016/S1164-0235(01)00009-7

[13] Torres, E., Navarrete, J.J. and Ibarra, B.A., Thermodynamic method for designing dryers operated by flat-plate solar collectors, Renew. Energy, 26, pp. 649-660, 2002. DOI: 10.1016/S0960-1481(01)00147-1

[14] Torres, E., Navarrete, J., Zaleta, A. and Cervantes-de Gortari, J.G., Optimal process of solar to thermal energy conversion and design of irreversible flat-plate solar collectors, Energy, 28(2), pp. 99-113, 2003. DOI: 10.1016/S0360-5442(02)00095-6

[15] Mortazavi A. and Ameri, M., Conventional and advanced exergy analysis of solar flat plate air collectors, Energy, 142, pp. 277-288, 2018. DOI: 10.1016/j.energy.2017.10.035

[16] Dasari, N. and Sridhar, K., A literature survey on thermodynamic analysis of a flat-plate solar air heater having different obstacles on absorber plate, The sun, 2017.

[17] El-Ferouali, H., Zoukit, A., Salhi, I., El Kiali, T., Doubabi, S. and Abdenouri, N., Thermal efficiency and exergy enhancement of solar air heaters, comparative study and experimental investigation, Journal of Renewable and Sustainable Energy 10(4), art. 043709, 2018. DOI: 10.1063/1.5039306

[18] Chauhan, R., Thakur, N.S., Singh, T. and Sethi, M., Exergy based modeling and optimization of solar thermal collector provided with impinging air jets, Journal of King Saud University-Engineering Sciences, 30(4), pp. 355-362, 2018. DOI: 10.1016/j.jksues.2016.07.003

[19] Hu, J., Liu, K., Ma, L. and Sun, X., Parameter optimization of solar air collectors with holes on baffle and analysis of flow and heat transfer characteristics, Solar Energy, 174, pp. 878-887, 2018. DOI: 10.1016/j.solener.2018.09.075

[20] Bakari, R., Heat transfer optimization in air flat plate solar collectors integrated with baffles, Journal of Power and Energy Engineering, 6(1), pp. 70-84, 2018. DOI: 10.4236/jpee.2018.61006

[21] Debnath, S., Reddy, J., Das, B. and Jagadish, Modeling and optimization of flat plate solar air collectors: an integrated fuzzy method, Journal of Renewable and Sustainable Energy, 11(4), art. 043706, 2019. DOI: 10.1063/1.5050896

[22] Cengel Y.A. and Boles, M.A., Thermodynamics an engineering approach, 8th Ed. McGraw-Hill Education, New York, USA, 2015.

[23] Khan, W.A., Culham, J.R. and Yovanovich, M.M., Optimization of pin-fin heat sinks in bypass flow using entropy generation minimization method, J. Electron. Packag., 130(3), pp. 653-661, 2008. DOI: 10.1115/IPACK2007-33983

[24] Cruz, M.M., Avina, J.G., Amaya, I.M. and Correa, R., Design of an optimal heat sink for microelectronic devices using entropy generation minimization, in: Proc. 14th Mex. Int. Conf. Artif. Intell. Adv. Artif. Intell. MICAI 2015, 2015, pp. 231-235. DOI: 10.1109/MICAI.2015.42

[25] de Silva, C., Mechatronic Systems, 15(3), SPEC. ISS. CRC Press, New York, USA, 2008.

[26] Culham J.R. and Muzychka, Y.S., Optimization of plate fin heat sinks using entropy generation minimization, in: IEEE Transactions on Components and Packaging Technologies, 24(2), pp. 159-165, 2001. DOI: 10.1109/6144.926378

[27] Shih, C. J. and Liu, G.C., Optimal design methodology of plate-fin heat sinks for electronic cooling using entropy generation strategy ,in: IEEE Trans. Components Packag. Technol., 27(3), pp. 551-559, 2004. DOI: 10.1109/TCAPT.2004.831812

[28] Cengel, Y.A., Heat transference a practical approach, 2nd d. 2002.

Notes

M.J. Muñoz-Neira, is BSc. in Electronic Engineer and MSc. in Electronic Engineering from the Universidad Industrial de Santander, Colombia. He is researcher associated to the Faculty of Engineering from Unisangil, San Gil, Colombia. His research interests include modeling, simulation and control of agro-industrial process, artificial intelligence, and teaching of basic science. ORCID: 0000-0001-6724-9888

M.F. Roa-Ardila, is BSc. in Chemist from Universidad Industrial de Santander, Colombia. He received his MSc. in Polímeros y Biopolímeros from Universitat Politècnica de Catalunya, España. At present time he is PhD. Candidate in Materials Engineering from Universidad Industrial de Santander. His research interests include thermogravimetry, polymer materials, nanomaterials, and thermal analysis. ORCID: 0000-0001-7777-9372

C.R. Correa-Cely, is BSc. in Chemical Engineering from Universidad Nacional de Colombia. He received his MSc. in Chemical Engineering from Universidad Industrial de Santander, UIS, Colombia, and his PhD. in Polymer Science and Engineering from Lehigh University, Bethlehem, PA, USA. He is full profesor from the Electric, Electronic and Telecommunications Department from UIS, Colombia. His research interests include control and simulation, polymers and new technologies. ORCID: 0000-0002-6507-1809

How to cite: Muñoz, M, Roa, M. and Correa, R, Entropy generation analysis for the Ddesign of a flat plate solar collector with fins. DYNA, 87(212), pp. 199-208, January - March, 2020.